

Interaction of excitons with a generalized Morse surface potential: *s*-polarized incident light at a semiconductor surface

F. Pérez-Rodríguez and P. Halevi

Instituto de Física de la Universidad Autónoma de Puebla, Apartado Postal J-48, Puebla, Pue. 72570, Mexico

(Received 17 December 1991)

Exciton reflection spectra of direct-band-gap semiconductors are investigated theoretically with the aid of an appropriate model for the surface potential. The dynamics of excitonic polaritons subject to a generalized Morse surface potential and the corresponding optical response are solved exactly for the *s*-polarization geometry. These calculations include an analytic determination of the profiles of the electric field and the polarization vector and of the reflectivity for *s*-polarized light. The correlation between the parameters of this extrinsic surface potential (height at the surface, width, depth of the well, and surface damping) and the reflectance spectra is studied for the *A* excitons of CdS and GaAs as examples. We also analyze the manifestation of near-surface localized excitons in the reflection line shape. It is demonstrated that the excitonic bound states cause broad peaks in the spectra.

I. INTRODUCTION

For many years the optical properties of undoped, direct-band-gap semiconductors (insulators in practice) in the excitonic region of frequencies have been intensively studied (see, for example, Refs. 1–6). At the present time, it is well established that the exciton reflection spectra are strongly sensitive to the state of the near-surface layer (transition layer).⁶ This fact is interpreted as a consequence of the interaction of excitons with a surface potential. The form of this potential depends on several factors: process of sample growth and special treatments of the crystal (illumination, doping, electron and ion bombardment, application of electric field, heating, etc.).

The transition layers of crystals may be classified in two groups.^{7,8} The first comprises intrinsic layers that repel excitons. The image potential^{2,9} and the no-escape condition for the electron and hole^{9,10} contribute to the formation of these layers. In the second group there are transition layers that have an extrinsic contribution (due to surface charges) to the surface potential. Depending on the characteristics of this contribution, the excitons may be attracted or repelled by the surface, and may also suffer additional absorption. Moreover, in these layers the exciton wave function and the polariton fields behave differently than in the bulk.⁸

In order to understand the correlation between the exciton reflection line shape and the nature of the transition layer, various theoretical models for the surface potential have been proposed. Hopfield and Thomas² suggested the model of the “exciton-free layer,” also called the “dead layer.” The essence of the exciton-free-layer model consists in the replacement of the intrinsic repulsive potential $U(z)$ by an impenetrable barrier (infinite step) at some distance $z=l$ from the surface. Sugakov and Khotyaintsev¹¹ supposed a linear dependence of the surface potential on the coordinates and solved exactly the problem of the motion of an exciton-polariton in a medium with spatial dispersion. A more realistic model to describe a repulsive layer is the exponential one:

$U(z) = U_0 \exp(-z/a)$ (U_0 and a are parameters). Assuming this exponential form of the potential, Skaistis and Khotyaintsev¹² found the exact solution to the exciton-polariton motion problem in the case of normal incidence. Balslev,¹³ Ruppin and Englman,¹⁴ and Ruppin¹⁵ also employed the exponential model; however, the results of their investigations were obtained from numerical calculations. The exponential potential explains well the experimental reflectivity spectra of both II-VI and III-V semiconductors.¹³

The presence of an extrinsic contribution to the surface potential is very common. This is due principally to the great facility of the transition layer to be modified by impurity ions which are produced with surface treatments or even unintentionally during the crystal growth. The impurities give rise to a near-surface macroscopic electric field and, as a result, a band bending.⁷ A fundamental investigation of the action of the near-surface electric field on excitons has been performed by Blossey.^{16,17} Evangelisti, Frova, and Patella⁷ examined the effect of the extrinsic layers on exciton reflectance, making use of the model of Hopfield and Thomas. They concluded that the impurities in the near-surface region increase the dead-layer thickness. In a series of works Kiselev,^{8,18–21} and Lagois²² analyzed the reflectivities corresponding to different models of the potential $U(z)$ with an attractive part. The potential was approximated by a multistep model. Also considered is a gradual increase of the exciton damping near the surface because of the probability of dissociation of the exciton due to impurities. A problem of current interest is the generation of bound excitonic states in the surface potential well.^{23,24} These states may manifest themselves in the reflection spectra as a complex structure of spikes. Thus important variations in the reflection line shape, owing to exciton localization at treated semiconductor surfaces, have been observed in several experimental works.^{25–28}

The principal purpose of the present work is to investigate the behavior of excitons, and the corresponding exciton-polaritons, with a realistic enough model for the

surface potential $U(z)$ which, at the same time, permits us to find an analytic solution to the problem. For this reason we have proposed a model for $U(z)$, named the generalized Morse surface potential, whose functional form is

$$U(z) = \begin{cases} U_1 e^{-z/a} + U_2 e^{-2z/a}, & z > 0 \\ \infty, & z < 0 \end{cases} \quad (1)$$

(the infinite half-space $z > 0$ is occupied by the semiconductor). The quantities U_1 , U_2 , and a are parameters that depend on the type of transition layer. Thus, in the cases $|U_1| \ll |U_2|$ or $|U_2| \ll |U_1|$ the model (1) is essentially exponential and describes repulsive potentials [see Fig. 1(a)], which are characteristic of intrinsic semiconductors at low temperatures. In more general cases $U(z)$ from (1) can be adjusted to represent shallow [Fig. 1(b)] or deep [Fig. 1(c)] potential wells. These potentials correspond to strongly treated surfaces. The conventional Morse potential is obtained by choosing $U_1 = -2U_2$ and by extending the validity of Eq. (1) (for $z > 0$) to all z .

Another objective of this paper is to find a detailed correlation between the physical parameters of the surface potential (height at the surface, and depth and width of the well) and the reflectivity spectra. Such a dependence can shed light on the form of $U(z)$ on the basis of experimental spectra, and ultimately can be related to the state of the sample surface. Moreover, it is of great interest to understand the connection between the spectral resonances (spikes) and the eigenstates of mechanical excitons, localized near the surface.

In Sec. II, using the generalized Morse surface potential, we obtain analytic exact expressions of the electric field and the excitonic polarization and of the semiconductor reflectivity for s -polarized light. The study of the influence of the potential parameters on the reflectivity spectra is carried out in Sec. III. Finally (Sec. IV), we investigate the form of manifestation of near-surface localized excitons in the reflectance.

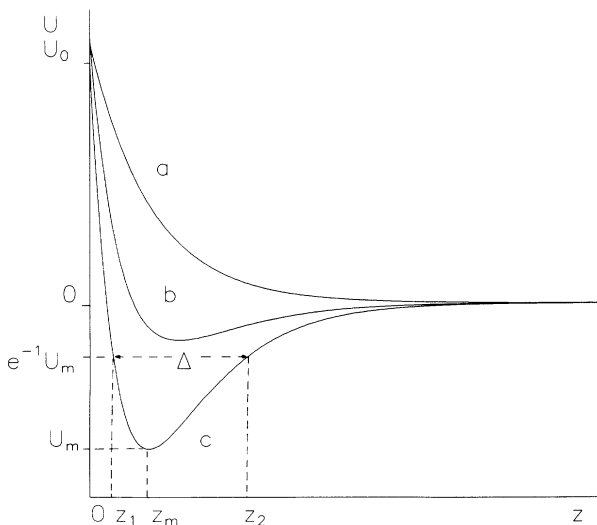


FIG. 1. Generalized Morse surface potential: a, exponential; b, shallow well; c, deep well.

This work is the first of a planned series devoted to the analysis of the interaction of excitons with the generalized Morse surface potential. A future paper will deal with p -polarized light incident at a surface. A third paper will be devoted to transmission by a thin film.

II. THEORY

Let us consider a spatially dispersive dielectric occupying the semispace $z > 0$. In the region $z < 0$, which corresponds to vacuum, the incident and reflected fields are s -polarized and have the form

$$\begin{aligned} \mathbf{E}_i &= (0, E_i(x, z, t), 0), \\ E_i(x, z, t) &= E_i e^{i(q_x x + q_z z) - i\omega t}, \\ \mathbf{E}_r &= (0, E_r(x, z, t), 0), \\ E_r(x, z, t) &= E_r e^{i(q_x x - q_z z) - i\omega t}, \end{aligned} \quad (2)$$

where

$$q_x = q \sin \theta, \quad q_z = q \cos \theta, \quad q = \omega/c, \quad (3)$$

ω is the frequency, θ is the angle of incidence, and c is the speed of light in vacuum.

In order to investigate the optical properties of nonlocal dielectrics, we will employ a system of coupled differential equations for the electric field and polarization vector in the medium ($z > 0$). This system is composed of the equation of motion for the polarization \mathbf{P} and the wave equation for the electric field \mathbf{E} . For the assumed geometry

$$\mathbf{P} = (0, P(x, z, t), 0), \quad P(x, z, t) = P(z) e^{i q_x x - i \omega t} \quad (4)$$

and the system of equation to solve is²

$$\begin{aligned} \left[\frac{\partial^2}{\partial z^2} + \Gamma^2(z) \right] P(z) &= -\frac{\omega_p^2 M}{4\pi \hbar \omega_T} E(z), \\ \left[q_x^2 - \epsilon_0 \frac{\omega^2}{c^2} - \frac{\partial^2}{\partial z^2} \right] E(z) &= \frac{4\pi \omega^2}{c^2} P(z), \end{aligned} \quad (5)$$

where

$$\begin{aligned} \Gamma^2(z) &= \Gamma_B^2 + \Delta \Gamma^2(z), \\ \Gamma_B^2 &= \frac{M}{\hbar \omega_T} \left[\omega^2 - \omega_T^2 - \frac{\hbar \omega_T}{M} q_x^2 + i \omega \nu \right], \\ \Delta \Gamma^2(z) &= -\frac{2 M U(z)}{\hbar^2}. \end{aligned} \quad (6)$$

$$(7)$$

Here $E(z)$ is the y component of the electric field in the region $z \geq 0$, ϵ_0 is the background dielectric constant, ω_T is the frequency of the exciton resonance, ω_p is a measure of the oscillator strength, ν is the damping constant, and M is the translational exciton mass.

It is important to mention that the excitonic polarization field \mathbf{P} in (4) is proportional to the exciton wave function of the translational motion and that the first equation in (5) was obtained by time-dependent perturbation theory for a single excitonic resonance.^{2,9} The sur-

face potential $U(z)$, which appears in Eqs. (5)–(7), in fact determines the shift of the binding energy of the electron-hole pair with respect to its bulk value [$\Delta E_{\text{binding}}(z) = -U(z)$].

Equations (5)–(7) are valid in the frequency region $|\omega - \omega_T| \ll \omega_T$. Hence the parameter Γ_B^2 can be “renormalized” such that it includes $\Delta\Gamma^2(z)$. Indeed, making the substitutions

$$\omega_T \rightarrow \omega_T(z) = \omega_T + \Delta\omega_T(z), \quad \Delta\omega_T(z) = \text{Re}U(z)/\hbar, \quad (8a)$$

$$v \rightarrow v(z) = v + \Delta v(z), \quad \Delta v(z) = -2 \text{Im}U(z)/\hbar,$$

in formula (7) for Γ_B^2 we find that $\Gamma^2(z)$ in (6) may be written as

$$\Gamma^2(z) \cong \frac{M}{\hbar\omega_T} \left[\omega^2 - \omega_T^2(z) - \frac{\hbar\omega_T}{M} q_x^2 + i\omega v(z) \right]. \quad (8b)$$

As has been commented in the Introduction we assume that the complex surface potential $U(z)$ in Eqs. (5)–(7) is given by the generalized Morse surface potential (1). This model has two complex parameters (U_1, U_2) and one real (a). In the particular case that $U_1 = -2U_2$ the potential $U(z)$ ($z > 0$) takes the form of the “classical” Morse potential truncated at $z = 0$.

The system of equations (5) can be reduced to one equation for $P(z)$ by substituting $E(z)$ from the first equation in (5) into the second one. We get

$$\begin{aligned} \frac{\partial^4}{\partial z^4} P + \left[\epsilon_0 \frac{\omega^2}{c^2} - q_x^2 + \Gamma^2(z) \right] \frac{\partial^2}{\partial z^2} P + 2 \frac{\partial \Gamma^2}{\partial z} \frac{\partial P}{\partial z} \\ + \left[\left[\epsilon_0 \frac{\omega^2}{c^2} - q_x^2 \right] \Gamma^2(z) - \frac{\omega_P^2 \omega^2 M}{c^2 \hbar \omega_T} + \frac{\partial^2 \Gamma^2}{\partial z^2} \right] P = 0. \end{aligned} \quad (9)$$

For the half-space $z > 0$ the function $P(z)$ can be written as a linear combination of only two independent solutions of Eq. (9):

$$P(z) = A_1 P_1(z) + A_2 P_2(z). \quad (10)$$

In the bulk [$\exp(-z/a) \ll 1$], where $\Delta\Gamma^2(z) \rightarrow 0$ and $\Gamma^2(z) \rightarrow \Gamma_B^2$, the functions $P_s(z)$ ($s = 1, 2$) have the asymptotic form

$$P_s(z) = e^{iq_s z}, \quad (11)$$

where q_s ($\text{Im}q_s > 0, s = 1, 2$) are

$$\begin{aligned} q_{1,2} = \left[\frac{1}{2} \left[\Gamma_B^2 + \epsilon_0 \frac{\omega^2}{c^2} - q_x^2 \pm \left[\left[\Gamma_B^2 - \epsilon_0 \frac{\omega^2}{c^2} + q_x^2 \right]^2 \right. \right. \right. \\ \left. \left. \left. + \frac{4\omega_P^2 \omega^2 M}{c^2 \hbar \omega_T} \right]^{1/2} \right] \right]^{1/2}. \end{aligned} \quad (12)$$

For arbitrary z it is convenient to write

$$P_s(z) \equiv e^{iq_s z} F_s(z), \quad (13)$$

where $F_s(z)$ are to be determined. For large values of z [$\exp(-z/a) \ll 1$] the functions $F_s(z)$ are practically constants [$F_s(z) \approx 1$].

After substitution of expressions (10) and (13) into Eq. (9) we obtain the equations for the functions $F_s(z)$ ($s = 1, 2$):

$$\begin{aligned} \frac{\partial^4 F_s}{\partial z^4} + 4iq_s \frac{\partial^3 F_s}{\partial z^3} + \left[6(iq_s)^2 + \Gamma_B^2 + \Delta\Gamma^2(z) + \epsilon_0 \frac{\omega^2}{c^2} - q_x^2 \right] \frac{\partial^2 F_s}{\partial z^2} \\ + \left[4(iq_s)^3 + 2iq_s \left[\Gamma_B^2 + \Delta\Gamma^2(z) + \epsilon_0 \frac{\omega^2}{c^2} - q_x^2 \right] + 2 \frac{\partial \Delta\Gamma^2(z)}{\partial z} \right] \frac{\partial F_s}{\partial z} \\ + \left[\Delta\Gamma^2(z) \left[(iq_s)^2 + \epsilon_0 \frac{\omega^2}{c^2} - q_x^2 \right] + 2iq_s \frac{\partial \Delta\Gamma^2(z)}{\partial z} + \frac{\partial^2 \Delta\Gamma^2(z)}{\partial z^2} \right] F_s = 0. \end{aligned} \quad (14)$$

These equations with the surface potential $U(z)$ from (1) may be solved exactly. Introducing the variable

$$\xi = e^{-z/a}, \quad (15)$$

and a set of functions $f_s(\xi)$ ($s = 1, 2$) defined by

$$f_s(\xi(z)) = F_s(z), \quad (16)$$

Equations (14) can be written in the form

$$\begin{aligned} \xi^4 \frac{\partial^4 f_s}{\partial \xi^4} + \alpha_{1s} \xi^3 \frac{\partial^3 f_s}{\partial \xi^3} + (\alpha_{2s} \xi^2 + \alpha_{3s} \xi^3 + \alpha_{4s} \xi^4) \frac{\partial^2 f_s}{\partial \xi^2} \\ + (\alpha_{5s} \xi + \alpha_{6s} \xi^2 + \alpha_{7s} \xi^3) \frac{\partial f_s}{\partial \xi} + (\alpha_{8s} \xi + \alpha_{9s} \xi^2) f_s = 0. \end{aligned} \quad (17)$$

Here the coefficients α_{is} ($i = 1, 2, \dots, 9; s = 1, 2$) are

$$\alpha_{1s} = 6 - 4\kappa_s,$$

$$\alpha_{2s} = 7 + \left[\Gamma_B^2 + \epsilon_0 \frac{\omega^2}{c^2} - q_x^2 \right] a^2 - 12\kappa_s + 6\kappa_s^2,$$

$$\alpha_{3s} = -\frac{U_1}{W}, \quad \alpha_{4s} = -\frac{U_2}{W},$$

$$\alpha_{5s} = 1 + \left[\Gamma_B^2 + \epsilon_0 \frac{\omega^2}{c^2} - q_x^2 \right] a^2 - 2\kappa_s \left[2 + \left[\Gamma_B^2 + \epsilon_0 \frac{\omega^2}{c^2} - q_x^2 \right] a^2 \right] + 6\kappa_s^2 - 4\kappa_s^3, \quad (18)$$

$$\alpha_{6s} = \frac{U_1}{W}(2\kappa_s - 3), \quad \alpha_{7s} = \frac{U_2}{W}(2\kappa_s - 5),$$

$$\alpha_{8s} = -\frac{U_1}{W} \left[1 + \left[\epsilon_0 \frac{\omega^2}{c^2} - q_x^2 \right] a^2 - 2\kappa_s + \kappa_s^2 \right],$$

$$\alpha_{9s} = -\frac{U_2}{W} \left[4 + \left[\epsilon_0 \frac{\omega^2}{c^2} - q_x^2 \right] a^2 - 4\kappa_s + \kappa_s^2 \right],$$

where

$$\kappa_s = \iota q_s a, \quad W = \hbar^2 / 2a^2 M. \quad (19)$$

Equations (17) may be solved by writing

$$f_s(\xi) = \sum_{k=0}^{\infty} a_{ks} \xi^k. \quad (20)$$

Insertion of this expression for $f_s(\xi)$ in Eq. (17) leads to the recursion relation

$$a_{k+1,s} = r_{ks} a_{ks} + t_{ks} a_{k-1,s} \quad (21)$$

for $k \geq 1$ with $a_{0s} = 1$ and $a_{1s} = -\alpha_{8s} / \alpha_{5s}$ ($s = 1, 2$). We have here

$$r_{ks} = -\frac{\alpha_{3s} k(k-1) + \alpha_{6s} k + \alpha_{8s}}{(k+1)[k(k-1)(k-2) + \alpha_{1s} k(k-1) + \alpha_{2s} k + \alpha_{5s}]}, \quad (22)$$

$$t_{ks} = -\frac{\alpha_{4s}(k-1)(k-2) + \alpha_{7s}(k-1) + \alpha_{9s}}{(k+1)[k(k-1)(k-2) + \alpha_{1s} k(k-1) + \alpha_{2s} k + \alpha_{5s}]}.$$

Using Eqs. (16) and (20), we express the functions $F_s(z)$ ($s = 1, 2$) as follows:

$$F_s(z) = \sum_{k=0}^{\infty} a_{ks} e^{-kz/a}. \quad (23)$$

The relations (10), (13), and (23) give us the solution $P(z)$ of Eq. (9) for the case of a dielectric half-space. With the aid of the first equation in (5) and the found polarization $P(z)$ we can write the electric field $E(z)$ in the form

$$E(z) = A_1 E_1(z) + A_2 E_2(z), \quad (24)$$

where

$$E_s(z) = -\frac{4\pi\hbar\omega_T}{\omega_p^2 M} e^{\iota q_s z} \left[\frac{\partial^2 F_s(z)}{\partial z^2} + 2\iota q_s \frac{\partial F_s(z)}{\partial z} + [\Gamma^2(z) - q_s^2] F_s(z) \right], \quad s = 1, 2. \quad (25)$$

At the surface of the dielectric we will apply Pekar's additional boundary condition (ABC) $P(0) = 0$.¹ This choice is justified by the finite radius of the Mott-Wannier exciton: the center of mass of the exciton cannot reach the surface plane $z = 0$, implying that the wave function (and polarization) there vanishes. The Pekar ABC and the first equation in (5) evaluated at $z = 0$ permit us to relate the constants A_1 and A_2 to the electric field at the surface $E(0)$. Thus,

where

$$A_1 = -\frac{\omega_p^2 M}{4\pi\hbar\omega_T} C_0 P_2(0) E(0), \quad (26)$$

$$A_2 = \frac{\omega_p^2 M}{4\pi\hbar\omega_T} C_0 P_1(0) E(0),$$

$$C_0 = [P_2(0)P_1''(0) - P_1(0)P_2''(0)]^{-1}. \quad (27)$$

Here the primes symbolize derivatives with respect to z . Employing the usual continuity conditions on the tangential components of the electric and magnetic fields at $z = 0$ we easily get the reflectivity

$$R = |r|^2, \quad r = \frac{E_r}{E_i} + \frac{\iota q_z - [E'(0)/E(0)]}{\iota q_z + [E'(0)/E(0)]}, \quad (28)$$

where, using Eq. (5),

$$\frac{E'(0)}{E(0)} = C_0 \{ P_2(0)[P_1'''(0) + \Gamma^2(0)P_1'(0)] - P_1(0)[P_2'''(0) + \Gamma^2(0)P_2'(0)] \}. \quad (29)$$

Finally, using the boundary condition $E(0) = E_i(1+r)$, we can express the fields $P(z)$ from (10) and $E(z)$ from (24) in terms of the incident-wave amplitude

$$P(z) = \frac{\omega_p^2 M}{4\pi\hbar\omega_T} C_0 [P_1(0)P_2(z) - P_2(0)P_1(z)](1+r)E_i, \quad (30)$$

$$E(z) = \frac{\omega_p^2 M}{4\pi\hbar\omega_T} C_0 [P_1(0)E_2(z) - P_2(0)E_1(z)](1+r)E_i.$$

Let us verify our results in the case of the repulsive exponential potential, which is a good model to represent surface potentials of sufficiently pure (intrinsic) semiconductors at very low temperatures.¹³ The exponential potential is a particular case of the generalized Morse surface potential. Thus, assuming that $U_2=0$ in (1) the function $U(z)$ becomes

$$U(z) = U_1 e^{-z/a}, \quad z > 0. \quad (31)$$

It is not difficult to demonstrate that with the repulsive potential (31) the functions $F_s(z)$ ($s=1,2$) in (23), which determine the effect of the surface potential on the fields $P(z)$ and $E(z)$ in (30), are expressed as

$$F_1(z) = {}_2F_3(1+\kappa_0-\kappa_1, 1-\kappa_1-\kappa_0; 1-\kappa_1+\kappa_2, 1-\kappa_1-\kappa_2, 1-2\kappa_1; \xi), \quad (32)$$

$$F_2(z) = {}_2F_3(1+\kappa_0-\kappa_2, 1-\kappa_2-\kappa_0; 1-\kappa_2+\kappa_1, 1-\kappa_2-\kappa_1, 1-2\kappa_2; \xi).$$

Here $\kappa_0 = (\epsilon_0)^{1/2} a \omega / c$, $\xi = (U_1/W)e^{-z/a}$, ${}_2F_3(a_1, a_2; b_1, b_2, b_3; \xi)$ is the generalized hypergeometric series. In the situation of normal incidence ($\theta=0$, $q_x=0$) the functions $F_s(z)$ from (32) go over into the corresponding results of the work.¹²

III. THE SURFACE POTENTIAL WITH EXTRINSIC CONTRIBUTION

In this section we will consider that the surface potential of the semiconductor has an attractive part due to the presence of impurities in the transition layer.⁸ Within our model [Eq. (1)], to simulate a real surface potential it is necessary to specify three parameters ($\text{Re}U_1, \text{Re}U_2, a$). We will relate them with quantities which characterize physically the potential (see Fig. 1): the height at the boundary U_0 , the minimum value U_m , and the width Δ defined as the difference between the roots z_2 and z_1 ($z_2 > z_1$) of the equation $\text{Re}U(z) = U_m e^{-1}$. Elementary calculations give us the dependences of $\text{Re}U_1$, $\text{Re}U_2$, and a on the physical parameters:

$$\text{Re}U_1 = U_0 - \text{Re}U_2,$$

$$\text{Re}U_2 = U_0 - 2U_m + [(U_0 - 2U_m)^2 - U_0^2]^{1/2}, \quad (33)$$

$$a = 0.4608\Delta.$$

The surface increment of the damping $\Delta\nu(z) = -2\text{Im}U(z)/\hbar$ will be described by an exponential function.²⁹ Taking U_2 as real we assume that the surface damping has a range a , namely,

$$\Delta\nu(z) = \Delta\nu_0 e^{-z/a}, \quad \Delta\nu_0 = -2\text{Im}U_1/\hbar. \quad (34)$$

Now let us analyze the theoretical results of calcula-

tions of normal incidence ($\theta=0$) reflectivity for the $A_{n=1}$ exciton of CdS. The CdS data used in the calculations are³⁰ $\hbar\omega_T = 2.55272$ eV, $\hbar\omega_p = 0.29396$ eV, $M = 0.94m$ (m is the free-electron mass), $\epsilon_0 = 9.1$, $\hbar\nu = 0.124$ meV (1 cm^{-1}). Figure 2 shows the modification of the reflection line shape with increasing width Δ of the surface potential well and fixing other parameters ($|U_m|$, U_0 , and $\Delta\nu_0$). Note that the increase of Δ diminishes the main reflection peak ($\omega \cong \omega_T$). Also, a spike appears near the longitudinal exciton frequency $\hbar\omega_L = 2.55458$ eV. Then the effect of "rotation" of the reflection contour with increase of Δ is obtained. Such a rotation has been reported in Ref. 31 for CdS samples treated by electron bombardment. Another important consequence of the variation of the width Δ (i.e., the extrinsic-transition-layer width) is the shift of the reflectance minimum R_{\min} to lower frequencies. The variation of other parameters (see Figs. 3–5) demonstrates that the redshift of R_{\min} is, fundamentally, due to the increment of Δ . The potential-well width is practically determined by the surface electric field, and may be found from the redshift observed in an experiment.

The reflectivity peak at ω_L is also obtained with increasing the depth of the potential well (see Fig. 3). This spike has been observed with doped CdS crystals in numerous experimental works.^{7,23,24} Moreover, in Fig. 3 the enhancement of the overall reflectivity is evident, contrary to the effect produced by the width increase (Fig. 2).

Variation of the height of the extrinsic surface potential (U_0) produces small changes in the reflectance spectra (see Fig. 4). However, these variations are different from those which are seen in the case of repulsive (intrinsic) potentials. There the effect of increasing U_0 leads to the reduction of the relative intensities of the main max-

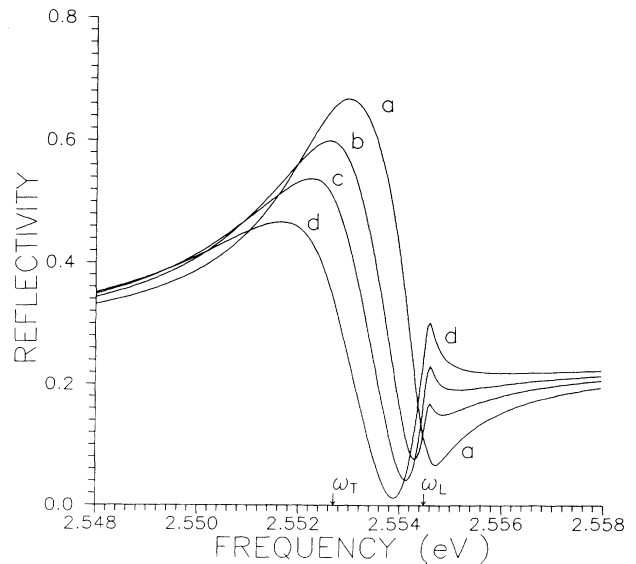


FIG. 2. Normal-incidence reflectivity of CdS with increasing the width Δ of the surface-potential well: a, 100 Å; b, 130 Å; c, 160 Å; d, 200 Å. Other parameters of the surface potential used are $U_0 = 4$ meV, $U_m = -2$ meV, $\hbar\Delta\nu_0 = 11$ meV.

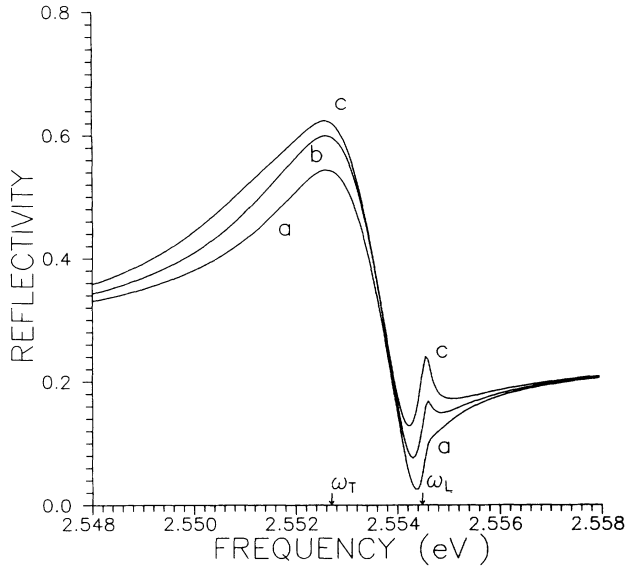


FIG. 3. Normal-incidence reflectivity of CdS with surface-potential parameters $\Delta=130 \text{ \AA}$, $U_0=4 \text{ meV}$, $\hbar\Delta\nu_0=11 \text{ meV}$; a , $U_m=-1 \text{ meV}$; b , $U_m=-2 \text{ meV}$; c , $U_m=-3 \text{ meV}$.

imum and minimum of the spectra, and to a small redshift of these extremes.¹⁵ Here (Fig. 4) the large maximum R_{\max} ($\omega \cong \omega_T$) is essentially unshifted. Thus the results of Fig. 4 cannot be explained by the existence of a repulsive potential near the semiconductor surface.

We know that the presence of impurities in the transition layer introduces an additional damping of the exciton-polariton, $\Delta\nu(z)$, due to the final probability of dissociation of the exciton in the surface electric field. The surface damping can considerably influence the

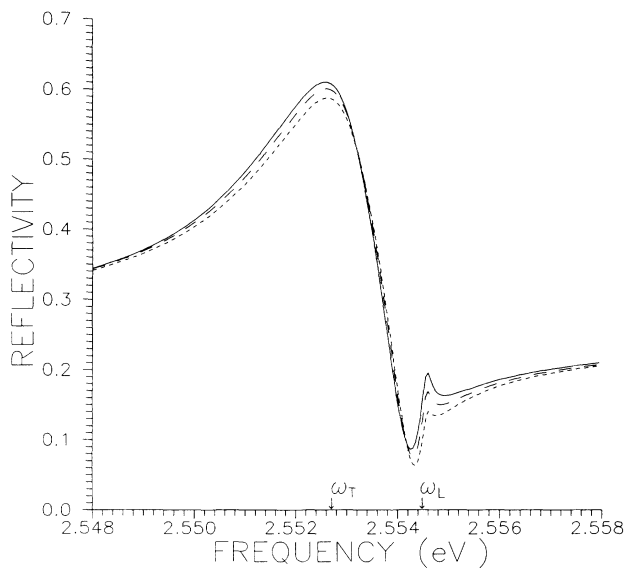


FIG. 4. Normal-incidence reflectivity of CdS for different heights of the extrinsic potential at the surface: $U_0=1 \text{ meV}$ (short-dashed line), $U_0=4 \text{ meV}$ (long-dashed line), $U_0=8 \text{ meV}$ (solid line). Other parameters used in the calculations are $\Delta=130 \text{ \AA}$, $U_m=-2 \text{ meV}$, $\hbar\Delta\nu_0=11 \text{ meV}$.

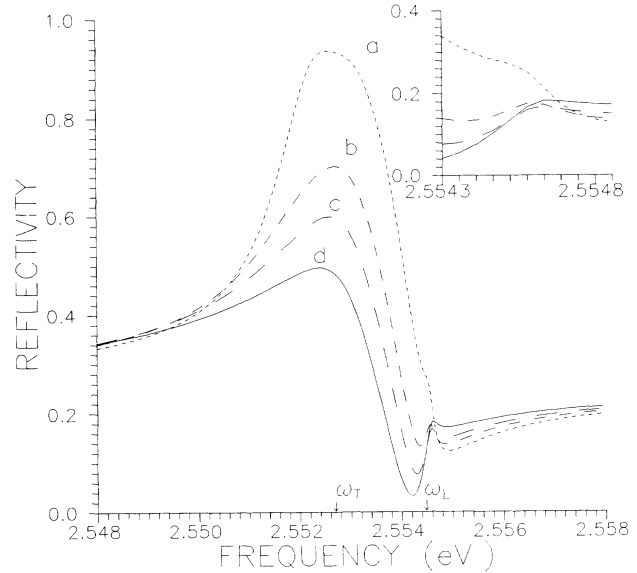


FIG. 5. Normal-incidence reflectivity of CdS with increasing surface damping: a , $\hbar\Delta\nu_0=0 \text{ meV}$; b , $\hbar\Delta\nu_0=6 \text{ meV}$; c , $\hbar\Delta\nu_0=11 \text{ meV}$; d , $\hbar\Delta\nu_0=20 \text{ meV}$. The parameters fixed are $U_0=4 \text{ meV}$, $U_m=-2 \text{ meV}$, $\Delta=130 \text{ \AA}$.

reflectivity spectra. Figure 5 shows the reflectance curves calculated for different values of the damping at the CdS surface, $\Delta\nu_0$. The enhancement of the main reflectance maximum ($\omega \cong \omega_T$) with decreasing the value of $\Delta\nu_0$ is very prominent. The shape of the spike at $\omega \cong \omega_L$ is also modified by the surface damping. So by increasing $\Delta\nu_0$, we can see in Fig. 5 that the spike is converted from a left spike (when the main reflectance minimum is at $\omega_{\min} > \omega_L$) to a right spike ($\omega_{\min} < \omega_L$). The left-to-right-spike conversion has been experimentally observed by increasing the doses of electron irradiation on the sample surface,²³ and with etching, too.³²

Now we will apply our theory to GaAs, which is a III-V semiconductor. Figures 6–8 show results of calculation of the GaAs reflectance. The GaAs data utilized were³³ $\hbar\omega_T=1.515 \text{ eV}$, $\hbar\omega_p=0.07106 \text{ eV}$, $\epsilon_0=12.6$, $\hbar\nu=0.035 \text{ meV}$. It should be pointed out that we consider a single exciton branch with mass $M=0.298m$, obtained by the average valence-band approximation.¹⁰

In Fig. 6 we show graphs of normal incidence reflectivity $R(\omega)$ for extrinsic surface potentials with distinct depths ($|U_m|$). In comparison to the CdS spectra it is evident that a “rotation” of the spectrum takes place for GaAs. As can be seen, there the increase of $|U_m|$ lowers more the main reflectance minimum R_{\min} ($\omega \cong \omega_T$) and, as in the case of II-VI semiconductors (see Fig. 2 for CdS), the spike at the frequency of the longitudinal exciton (ω_L) gradually becomes a prominent maximum.

The influence of Δ on the reflectance of GaAs (see Fig. 7) has some characteristics of the II-VI semiconductors spectra. For this reason, we can conclude that for both types (II-VI and III-V) of semiconductors the redshift of R_{\min} is an effect produced principally by the variation of the potential-well width, which is intimately related to

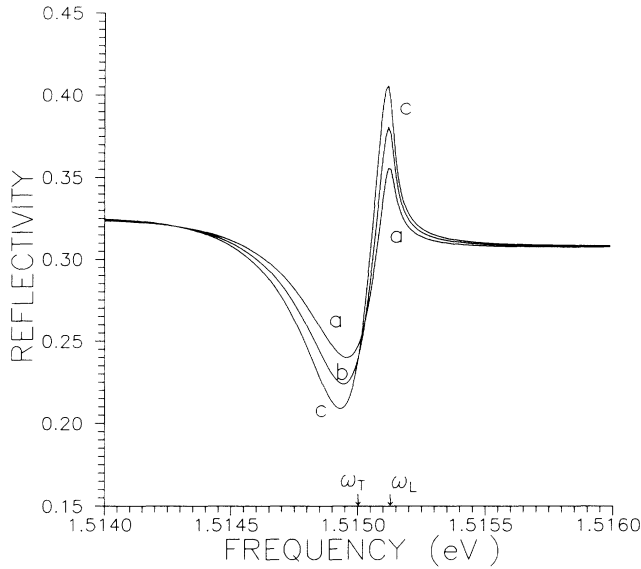


FIG. 6. Normal-incidence reflectivity of GaAs with surface-potential parameters $U_0=1$ meV, $\Delta=630$ Å, $\hbar\Delta\nu_0=2$ meV; a, $U_m=-0.05$ meV; b, $U_m=-0.1$ meV; c, $U_m=-0.15$ meV.

the penetration depth of the surface electric field originated by impurities.⁸

We have also analyzed the dependence $R(\omega)$ for GaAs with various angles of incidence. The graphs of reflectivity, obtained with the help of our method, are given in Fig. 8. As can be noted the spectra of oblique incidence for s polarization have similar features to the case of normal incidence reflectivity. Figure 8 also shows that the reflectivity R grows with increasing angle θ .

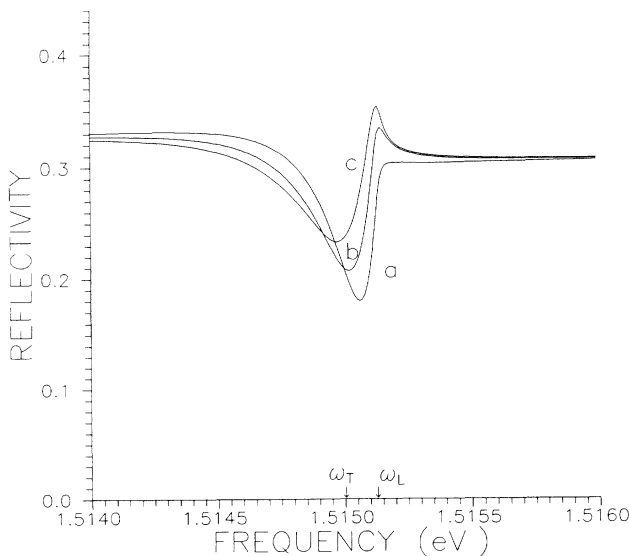


FIG. 7. Normal-incidence reflectivity of GaAs for different values of the well width Δ : a, 400 Å; b, 500 Å; c, 600 Å. Other potential parameters used: $U_0=1$ meV, $U_m=-0.05$ meV, $\hbar\Delta\nu_0=2$ meV.

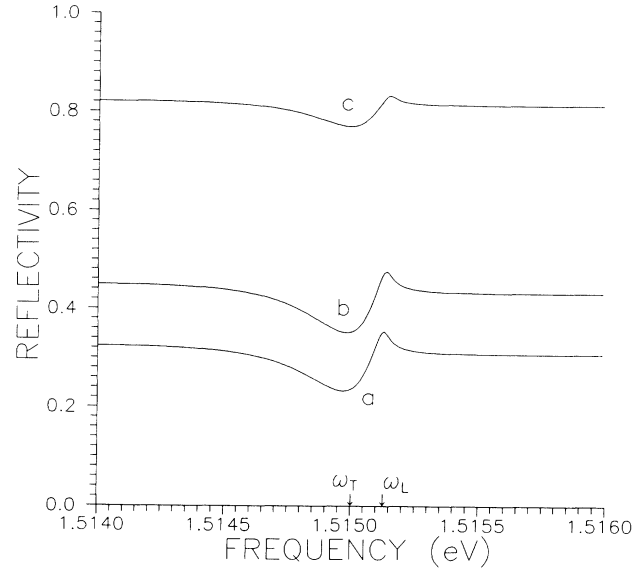


FIG. 8. Oblique-incidence reflectivity of GaAs for s -polarization a, $\theta=0^\circ$; b, $\theta=45^\circ$; c, $\theta=80^\circ$; and with $U_0=1$ meV, $U_m=-0.05$ meV, $\hbar\Delta\nu_0=2$ meV, $\Delta=600$ Å.

IV. LOCALIZATION OF EXCITONS AND ITS OPTICAL MANIFESTATION

In the Introduction we have commented that the surface potential well can give rise to excitonic bound states. In the present section we will study the influence of these states on these states on the reflectivity spectra. With this aim let us determine, first, the eigenvalues of energy $\hbar\omega_n$ ($n=1,2,\dots$) of mechanical exciton bound states for a specific potential well. We shall employ the Morse surface potential $U(z)$ from (1) with $U_1=-2U_2$, that is, the truncated Morse potential. In this case the function (1) can be written in terms of the minimum value U_m and the position of the minimum z_m [$U_m=U(z_m)$], as follows:

$$U(z)=|U_m|(e^{-2(z-z_m)/a}-2e^{-(z-z_m)/a}), \quad z>0. \quad (35)$$

The Schrödinger equation for the translational motion of excitons in the semispace $z>0$ is⁶

$$\left[\frac{\partial^2}{\partial z^2} + \frac{2M}{\hbar^2} [\hbar\omega - \hbar\omega_T - U(z)] \right] \psi(z) = 0. \quad (36)$$

The boundary conditions for the wave function $\psi(z)$ are

$$\psi(0)=0, \quad \psi(\infty)=0. \quad (37)$$

In the interval of energies $\hbar\omega_T - |U_m| < \hbar\omega < \hbar\omega_T$ (inside the potential well), Eq. (36) with the potential $U(z)$ from (35) has solutions of the form

$$\psi = C e^{-z/a} \phi(\xi), \quad (38)$$

where C is a constant, and

$$\phi(\xi) = \sum_{k=0}^{\infty} a_k \xi^k, \quad \xi = e^{-z/a}. \quad (39)$$

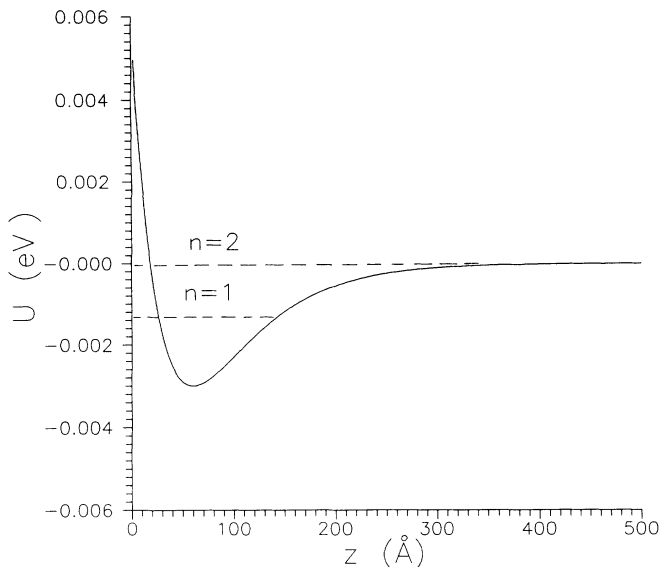


FIG. 9. Graph of the Morse surface potential with $U_m = -3$ meV, $z_m = 60$ Å, $a = 60$ Å. There are only two exciton bound states ($n = 1, 2$).

The coefficients a_k in Eq. (39) satisfy the recursion relation

$$a_{k+1} = v_m^2 \frac{e^{2z_m/a} a_{k-1} - 2e^{z_m/a} a_k}{(k+1)(2v+1+k)} \quad (40)$$

for $k \geq 1$, and with $a_0 = 1$ and $a_1 = -2v_m^2 \exp(z_m/a)(2v+1)^{-1}$. In expressions (38) and (40) we have introduced the quantities

$$\begin{aligned} v &= a [2M(\omega_T - \omega)/\hbar]^{1/2}, \\ v_m &= (a/\hbar)(2M|U_m|)^{1/2}. \end{aligned} \quad (41)$$

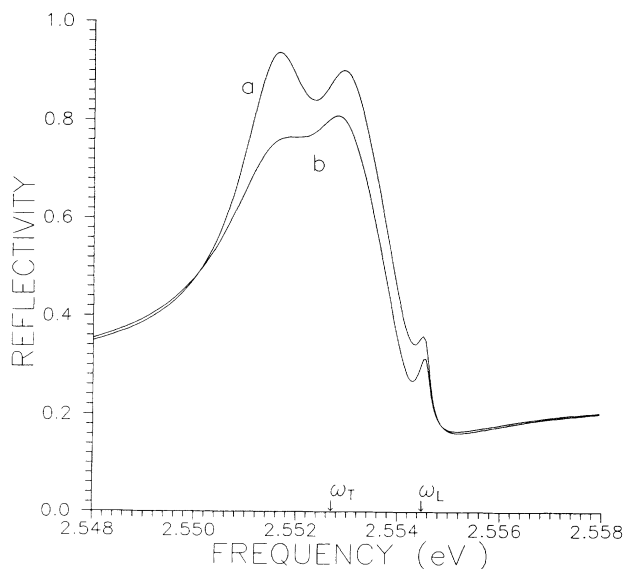


FIG. 10. Normal reflectance of CdS with the Morse surface potential shown in Fig. 9, and with a , $\hbar \Delta v_0 = 0$; b , $\hbar \Delta v_0 = 1$ meV.

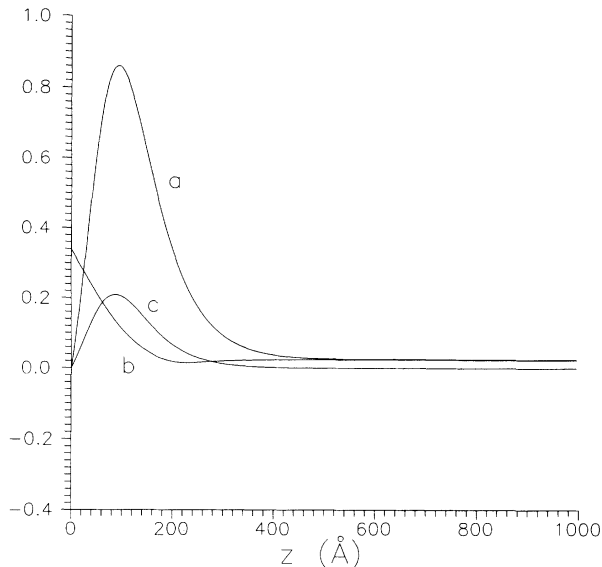


FIG. 11. Graphs of the absolute values of a , the excitonic polarization $|P(z)/E_i|$ and b , the electric field $|E(z)/E_i|$ for the Morse surface potential showed in Fig. 9, and with $\Delta v_0 = 0, \omega = \omega_{m1}$. Curve c is the exciton wave function $\psi_1(z)/C_1$ (see text). The other parameters correspond to CdS.

The eigenvalues $\hbar\omega_n$ are calculated by solving numerically the first equation in (37) [$\psi(0)=0$] with respect to ω . The number of eigenstates for the well of the Morse surface potential is finite.

Now we shall analyze the CdS normal reflectance for a Morse surface potential with exciton bound states. The parameters of the chosen potential (see Fig. 9) are $|U_m| = 3$ meV, $z_m = 60$ Å, and $a = 60$ Å. In this situation there are only two eigenvalues ($\hbar\omega_1 = 2.55137$ eV and

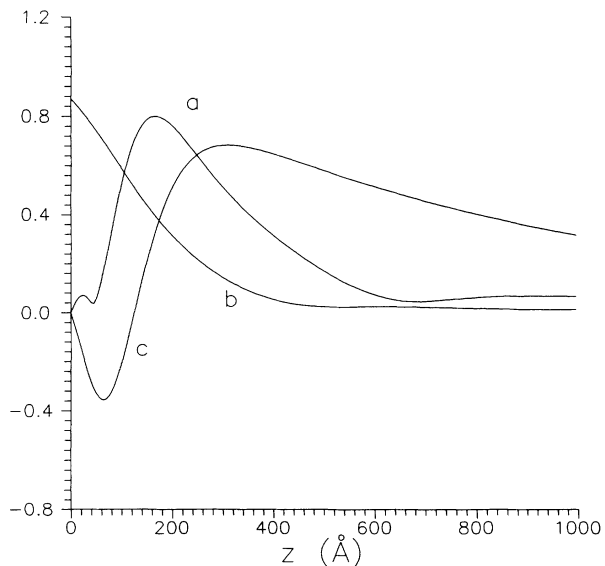


FIG. 12. Graphs of the absolute values of a , the excitonic polarization $|P(z)/E_i|$ and b , the electric field $|E(z)/E_i|$ for the Morse surface potential shown in Fig. 9, and with $\Delta v_0 = 0, \omega = \omega_{m2}$. Curve c is the exciton wave function $\psi_2(z)/C_2$ (see text). The other parameters correspond to CdS.

$\hbar\omega_2 = 2.55271$ eV) of excitonic bound states within the well. Reflectivity spectra corresponding to this potential (without and with surface damping) are presented in Fig. 10 (the CdS data are the same as those used in Sec. III). The bound states manifest themselves in the spectra as maxima at the frequencies $\omega_{m1} \cong (2.5516 \text{ eV}/\hbar)$, $\omega_{m2} \cong (2.5529 \text{ eV}/\hbar)$. The fact that the frequencies of the maxima are greater than the eigenvalues is a result of the interaction between the localized mechanical excitons and the electromagnetic fields in the medium (polariton effect³⁴). As may be expected, the surface damping (see curve *b*) diminishes the peaks gotten in its absence (curve *a*).

It is interesting to study the effect of the near-surface localized excitons on the excitonic polarization $P(z)$ and the electric field $E(z)$. Figures 11 and 12 show the results of calculating $|P(z)|$ and $|E(z)|$ at the frequencies ω_{m1}, ω_{m2} of the peaks in Fig. 10. In Figs. 11 and 12 we have also included the wave functions $\psi_1(z), \psi_2(z)$ of the exciton eigenstates (ω_1, ω_2). Note that the polarization field preserves important characteristics of the mechanical-exciton wave function. Thus $|P(z)|$ has one and two maxima for the first and the second bound state, respectively. Moreover, the excitonic polarization is strongly localized near the surface, in the well. These facts confirm that the broad peaks in the reflectance spectra (Fig. 10) are originated by localized excitons. Accord-

ing to Figs. 11 and 12, the electric field decreases in the surface potential well. This explains the manifestation of exciton bound states in the reflectance as a structure of maxima. CdS reflectance spectra with two peaks at frequencies $\omega_n < \omega_T$ ($n = 1, 2$) were observed in Ref. 27.

V. CONCLUSION

We have developed a theory which describes the influence of extrinsic-semiconductor surface potentials on the reflectivity spectra of *s* polarization. We found the principal effects produced by the variation of the surface-potential parameters and by the localization of excitons near the semiconductor surface. These results should be useful for inferring potential shapes from experimental spectra. However, because of large number of quantities to define, a reflectance spectrum can be reproduced by different sets of parameters. Consequently, for a satisfactory determination of the surface potential the parameters should be adjusted to the results of several experiments (for example, at distinct polarizations and angles of incidence) with the same sample.

ACKNOWLEDGMENTS

This work was partially supported by the Consejo Nacional de Ciencia y Tecnología (CONACyT).

-
- ¹S. I. Pekar, Zh. Eksp. Teor. Fiz. **33**, 1022 (1957) [Sov. Phys. JETP **6**, 785 (1958)].
- ²J. J. Hopfield and D. G. Thomas, Phys. Rev. **132**, 563 (1963).
- ³J. L. Birman, in *Excitons*, edited by E. I. Rashba and M. D. Sturge (North-Holland, Amsterdam, 1982), p. 72.
- ⁴S. I. Pekar, *Crystal Optics and Additional Light Waves* (Benjamin/Cummings, Menlo Park, CA, 1983).
- ⁵V. M. Agranovich and V. L. Ginzburg, *Crystal Optics with Spatial Dispersion, and Excitations* (Springer, Berlin, 1984).
- ⁶P. Halevi, in *Spatial Dispersion in Solids and Plasmas*, edited by P. Halevi (Elsevier, Amsterdam, in press).
- ⁷F. Evangelisti, A. Frova, and F. Patella, Phys. Rev. B **10**, 4253 (1974).
- ⁸V. A. Kiselev, Fiz. Tverd. Tela Leningrad **21**, 1069 (1979) [Sov. Phys. Solid State **21**, 621 (1979)].
- ⁹I. Balslev, Phys. Status Solidi B **88**, 155 (1978).
- ¹⁰A. D'Andrea and R. Del Sole, Phys. Rev. B **25**, 3714 (1982).
- ¹¹V. I. Sugakov and V. N. Khotyaintsev, Zh. Eksp. Teor. Fiz. **70**, 1566 (1976) [Sov. Phys. JETP **43**, 817 (1976)].
- ¹²E. G. Skaistis and V. N. Khotyaintsev, Fiz. Tverd. Tela Leningrad **24**, 3648 (1982) [Sov. Phys. Solid State **24**, 2079 (1982)].
- ¹³I. Balslev, Phys. Rev. B **23**, 3977 (1981).
- ¹⁴R. Ruppin and R. Englman, Phys. Rev. Lett. **53**, 1688 (1984).
- ¹⁵R. Ruppin, Phys. Rev. B **29**, 2232 (1984).
- ¹⁶D. F. Blossey, Phys. Rev. B **2**, 3976 (1970).
- ¹⁷D. F. Blossey, Phys. Rev. B **3**, 1382 (1971).
- ¹⁸V. A. Kiselev, Fiz. Tverd. Tela Leningrad **20**, 2173 (1978) [Sov. Phys. Solid State **20**, 1255 (1978)].
- ¹⁹V. A. Kiselev, Pis'ma Zh. Eksp. Teor. Fiz. **29**, 369 (1979) [JETP Lett. **29**, 332 (1979)].
- ²⁰V. A. Kiselev, Fiz. Tverd. Tela Leningrad **23**, 3680 (1981) [Sov. Phys. Solid State **23**, 2139 (1981)].
- ²¹V. A. Kiselev, Solid State Commun. **43**, 471 (1982).
- ²²J. Lagois, Phys. Rev. B **23**, 5511 (1981).
- ²³V. A. Kiselev, B. V. Novikov, A. E. Cherednichenko, and E. A. Ubushiev, Phys. Status Solidi B **133**, 573 (1986).
- ²⁴V. A. Kiselev, B. V. Novikov, A. S. Batyrev, E. A. Ubushiev, and A. E. Cherednichenko, Phys. Status Solid B **135**, 597 (1986).
- ²⁵V. A. Zuev, D. V. Korbutyak, M. V. Kurik, V. G. Litovchenko, A. Kh. Rozhko, and P. A. Skubneko, Pis'ma Zh. Eksp. Teor. Fiz. **26**, 455 (1977) [JETP Lett. **26**, 327 (1977)].
- ²⁶A. S. Batyrev, V. A. Kiselev, B. V. Novikov, and A. E. Cherednichenko, Pis'ma Zh. Eksp. Teor. Fiz. **39**, 436 (1984) [JETP Lett. **39**, 528 (1984)].
- ²⁷B. V. Novikov, E. A. Ubushiev, and A. E. Cherednichenko, Fiz. Tverd. Tela Leningrad **27**, 1359 (1985) [Sov. Phys. Solid State **27**, 821 (1985)].
- ²⁸V. A. Kiselev, B. V. Novikov, S. S. Utnasunov, and A. E. Cherednichenko, Fiz. Tverd. Tela Leningrad **28**, 2946 (1986) [Sov. Phys. Solid State **28**, 1655 (1986)].
- ²⁹L. Schultheis and J. Lagois, Phys. Rev. B **29**, 6784 (1984).
- ³⁰P. Y. Yu and F. Evangelisti, Phys. Rev. Lett. **42**, 1642 (1979).
- ³¹G. V. Benemanskaya, B. V. Novikov, and A. E. Cherednichenko, Fiz. Tverd. Tela Leningrad **19**, 1389 (1977) [Sov. Phys. Solid State **19**, 806 (1977)].
- ³²M. S. Brodin, A. V. Kirtskii, E. N. Myasnikov, M. I. Strashnikova, and L. A. Shlyakhova, Ukr. Fiz. Zh. **18**, 828 (1973).
- ³³A. D'Andrea and R. Del Sole, Phys. Rev. B **38**, 1197 (1988).
- ³⁴V. A. Kiselev, Fiz. Tverd. Tela Leningrad **20**, 1191 (1978) [Sov. Phys. Solid State **20**, 685 (1978)].